Hindawi Publishing Corporation
EURASIP Journal on Advances in Signal Processing
Volume 2007, Article ID 27427, 13 pages
doi:10.1155/2007/27427

Research Article

Construction of Orthonormal Piecewise Polynomial Scaling and Wavelet Bases on Non-Equally Spaced Knots

Anissa Zergaïnoh,[1,2] Najat Chihab,[1] and Jean Pierre Astruc[1]

[1] *Laboratoire de Traitement et Transport de l'Information (L2TI), Institut Galilée, Université Paris 13, Avenue Jean Baptiste Clément, 93 430 Villetaneuse, France*
[2] *LSS/CNRS, Supélec, Plateau de Moulon, 91 192 Gif sur Yvette, France*

Received 6 July 2006; Revised 29 November 2006; Accepted 25 January 2007

Recommended by Moon Gi Kang

This paper investigates the mathematical framework of multiresolution analysis based on irregularly spaced knots sequence. Our presentation is based on the construction of nested nonuniform spline multiresolution spaces. From these spaces, we present the construction of orthonormal scaling and wavelet basis functions on bounded intervals. For any arbitrary degree of the spline function, we provide an explicit generalization allowing the construction of the scaling and wavelet bases on the nontraditional sequences. We show that the orthogonal decomposition is implemented using filter banks where the coefficients depend on the location of the knots on the sequence. Examples of orthonormal spline scaling and wavelet bases are provided. This approach can be used to interpolate irregularly sampled signals in an efficient way, by keeping the multiresolution approach.

1. INTRODUCTION

Since the last decade, the development of the multiresolution theory has been extensively studied (see, e.g., [1–4]). Many science and engineering fields exploit the multiresolution approach to solve their application problems. Multiresolution analysis is known as a decomposition of a function space into mutually orthogonal subspaces. The specific structure of the multiresolution provides a simple hierarchical framework for interpreting the signal information. The scaling and wavelet bases construction is closely related to the multiresolution analysis. The standard scaling or wavelet basis is defined as a set of translations and dilations of one prototype function. The derived functions are thus self-similar at different scales. Initially, the multiresolution theory has been mainly developed within the framework of a uniform sample distribution (i.e., constant sampling time). The proposed scaling and wavelet bases, in the literature, are built under the assumptions that the knots of the infinite sequence to be processed are regularly spaced. However, the nonuniform sampling situation arises naturally in many scientific fields such as geophysics, astronomy, meteorology, medical imaging, computer vision. The data is often generated or measured at sparse and irregular positions. The majority of the theoretical tools developed in digital signal processing field are based on a uniform distribution of the samples. Many mathematical tools, such as Fourier techniques, are not adapted to this irregular data partition. The situation becomes much more complicated. It is within this framework that we concentrate our study. The non-equally spaced data hypotheses result in a more general definition of the scaling and wavelet functions. The authors of [5] have originally presented a theoretical study to perform a multiresolution analysis using the cardinal spline approach to the wavelets of arbitrary degree. The wavelet is given as the $(n+1)$th order derivative of the spline function of degree $2n+1$. The support of the wavelet is given by the interval $[x_i, x_{i+2n+1}]$ where x_k specifies the data position. The authors of paper [6] reviewed and discussed some techniques and tools for constructing wavelets on irregular set of points by means of generalized subdivision schemes and commutation rules. As a sequel of paper [6], the authors of [7] proposed the construction of a biorthogonal compactly supported irregular knot B-spline wavelet family. In paper [8], the authors investigated the construction of semiorthogonal spline scaling and wavelet bases on a bounded interval. They proposed the construction of nonuniform B-spline functions with multiple knots at each end points of the interval as special boundary

functions. The development of the scaling and wavelet bases, provided in this paper, focuses on piecewise polynomials, namely, nonuniform B-spline functions. These functions are widely used to represent curves and surfaces [9, 10]. They are well adapted to a bounded interval when a multiplicity of a given order is imposed on each end points of the definition domain of the nonuniform B-spline function [9]. The generated polynomial spline spaces allow an obviously scaling of the spaces as required for a multiresolution construction. Indeed a piecewise polynomial of a given degree, over a bounded interval, is also a piecewise polynomial over subinterval. Moreover, for such spline spaces, simple basis can be constructed. The proposed study is carried out within the framework of future investigation in the topic of recovering a discrete signal from its irregularly spaced samples in an efficient way by keeping the multiresolution approach. The construction of the scaling and wavelet bases on irregular spacing knots is more complicated than the traditional case (equally spaced knots). On a non-equally spaced knots sequence, we show that the underlying concept of dilating and translating one unique prototype function allowing the construction of the scaling and wavelet bases is not valid any more. The main objective of this paper is to provide, for this nontraditional configuration of knots sequence, a generalization of the underlying scaling and wavelet functions, yielding therefore an easy multiresolution structure.

This paper is organized as follows. Section 2 summarizes some necessary background material concerning the nonuniform spline functions allowing the design of orthonormal spline basis. Section 3 introduces the multiresolution spaces on bounded intervals. The construction of the corresponding orthonormal spline scaling basis is then developed, whatever the degree of the spline function. A generalization of the two scale equation is deduced. Section 4 introduces the wavelet spaces and gives the required conditions to design an orthonormal spline wavelet basis on bounded intervals. Explicit generalization of the wavelet bases is provided for any arbitrary degree of the spline function. Some examples are presented. Section 5 presents the orthogonal decomposition and reconstruction algorithm adapted to irregularly spaced data. Section 6 concludes the work.

2. ORTHONORMAL NONUNIFORM SPLINE BASIS ON BOUNDED INTERVALS

This section presents the orthonormal spline basis before undertaking the construction of the scaling and wavelet bases. Among the large family of piecewise polynomials available in the literature, the nonuniform B-spline functions have been selected because they provide many interesting properties (see, e.g., [9]). We start with reviewing the basic nonuniform B-spline function definition. Initially Curry and Schoenberg have proposed the nonuniform B-spline definition [9]. Consider a sequence S_0 composed of irregularly spaced known knots, organized according to an increasing order, as follows:

$$\tau_0 < \tau_1 < \cdots < \tau_i < \tau_{i+1} < \cdots . \tag{1}$$

Given a set of $d+2$ arbitrary known knots, the ith nonuniform B-spline function, denoted $B^d_{i,[\tau_i,\tau_{i+d+1}]}(t)$, is represented by a piecewise polynomial of degree d. Defined on the bounded interval $[\tau_i, \tau_{i+d+1}]$, the ith B-spline function is given by the following formula:

$$B^d_{i,[\tau_i,\tau_{i+d+1}]}(t) = (\tau_{i+d+1} - \tau_i)[\tau_i, \ldots, \tau_{i+d+1}](\cdot - t)^d_+. \tag{2}$$

This last equation is based on the $(d+1)$th divided difference applied to the function $(\cdot - t)^d_+$. Remember the divided difference definition

$$\begin{aligned}&[\tau_i, \ldots, \tau_{i+d+1}](\cdot - t)^d_+ \\ &\quad = (\tau_{i+d+1} - \tau_i)^{-1} \times \left([\tau_{i+1}, \ldots, \tau_{i+d+1}](\cdot - t)^d_+ \right. \\ &\qquad \left. - [\tau_i, \ldots, \tau_{i+d}](\cdot - t)^d_+\right),\end{aligned} \tag{3}$$

where $(x-t)_+ = \max(x-t, 0)$ is the truncation function.

If a knot in the increasing knot sequence S_0 has a multiplicity of order $\mu+1$, that is, the knot occurs $\mu+1$ times $(\tau_i <= \cdots <= \tau_{i+\mu})$, then the definition of the divided difference applied to the function $g = (\cdot - t)^d_+$ becomes

$$[\tau_i, \ldots, \tau_{i+\mu}]g = g^{(\mu)}(\tau_i)/\mu! \quad \text{if } \tau_i = \cdots = \tau_{i+\mu}. \tag{4}$$

It has been shown that the set of n nonuniform B-spline functions, $\{B^d_{i,[\tau_i,\tau_{i+d+1}]}, \ldots, B^d_{i+n-1,[\tau_{i+n-1},\tau_{i+n+d}]}\}$, defined on the knots sequence $a = \tau_i < \tau_{i+1} < \cdots < \tau_{i+d+n} = b$, generates a basis for the spline space spanned by polynomials of degree d. The linear combination of these n B-spline functions defines the spline function. The dimension n of the basis depends on the multiplicities imposed on each knot of the sequence [9]. Hence, for a fixed degree of the spline function, several bases of different dimensions can be built. In previous works, we have shown that the smallest interpolation error is carried out for the basis of the smallest dimension, that is, $d+1$ [9, 11]. This involves imposing a multiplicity of order $d+1$ on each knot of the sequence. So, the increasing sequence S_0 becomes now

$$\begin{aligned}\tau_0 = \tau_1 = \cdots = \tau_d < \cdots < \tau_i = \tau_{i+1} = \cdots \\ = \tau_{i+d} < \tau_{i+1+d} = \tau_{i+2+d} = \cdots = \tau_{i+1+2d} \\ < \tau_{i+2+2d} = \tau_{i+3+2d} = \cdots = \tau_{i+2+3d} < \cdots .\end{aligned} \tag{5}$$

For writing convenience reasons, the knots of the sequence S_0 are renamed to be used in the next sections as follows:

$$t_{i+k} = \tau_{i+k(d+1)} = \cdots = \tau_{i+k(d+1)+d} \quad \text{for } k \in N. \tag{6}$$

According to these notations, the sequence S_0 is denoted as follows:

$$t_0 < \cdots < t_i < t_{i+1} < t_{i+2} < \cdots . \tag{7}$$

The spline definition domain is thus reduced to the following bounded interval $[t_i, t_{i+1}]$. Meaning that the $d+1$ B-spline functions are defined between two consecutive knots $[t_i, t_{i+1}]$. This particular B-spline is known in the literature as Bernstein function [9]. Our study is based on this configuration of knots. The generalized expression of the nonuniform B-spline function, whatever the spline degree, is given by the

following equation [9, 10]:

$$B^d_{k,[t_i,t_{i+1}]}(t) = C^i_d \left(\frac{t_{i+1}-t}{t_{i+1}-t_i}\right)^{d-k} \left(\frac{t-t_i}{t_{i+1}-t_i}\right)^k \quad \text{for } t_i \le t < t_{i+1},\ 0 \le k \le d, \tag{8}$$

where $C^k_d = d!/k!(d-k)!$ is the binomial coefficient.

The important drawback of these particular piecewise polynomials is the discontinuity of the functions (8) between adjacent intervals. As it will be developed in the next sections, the process of decomposing and reconstructing a signal is however simplified with these functions. Of course, many other choices are possible concerning the multiplicity of knots but at the detriment of (i) an important computational cost when going from one resolution level to another one; and (ii) a larger interpolation error as shown in [11].

In order to construct an orthonormal spline basis, we propose to use the traditional Gram-Schmidt method. The orthonormal spline basis is therefore not unique since one can choose different nonuniform B-spline as the first reference component for the Gram-Schmidt method. The orthonormal spline basis elements are denoted $\{\underline{B}^d_{k,[t_i,t_{i+1}]}(t)\}$. The basic spline space spanned by piecewise polynomials of degree d is denoted V_0. It is given as follows:

$$V_0 = \text{span}\,\{\underline{B}^d_{k,[t_i,t_{i+1}]}(t)\ \forall k \in [0,d];\ \forall i \in N\}. \tag{9}$$

3. SPLINE SCALING FUNCTION IRREGULAR PARTITION OF KNOTS

This section focuses on a generalized construction of the orthonormal spline scaling basis, whatever the spline function degree under the assumptions of an irregular partition of the knots sequence. We begin by introducing some definitions and notations.

3.1. Notations

Consider an initial infinite knots sequence S_0 organized as follows $t_0 < t_1 < \cdots < t_i < t_{i+1} < \cdots$. Remember that a multiplicity of order $d+1$ is imposed on each knot of the sequence S_0 (see (6)). This one is considered as the finest sequence representing a non-equally spaced knots partition. Let us first denote $I_{j,i}$ the bounded interval, at any given resolution level j as follows:

$$I_{j,i} = [t_{2^j i}, t_{2^j(i+1)}[. \tag{10}$$

The corresponding knots sequence at resolution level j is denoted S_j. It is thus built from the union of bounded intervals $I_{j,i}$ as defined below:

$$S_j = \bigcup_{i=0}^{\infty} I_{j,i} \quad \text{with } i \in N. \tag{11}$$

Going from the resolution level $j-1$ to the resolution level j (coarse resolution) consists in removing one knot out of two from the sequence S_{j-1}. Hence, we obtain obviously a set of embedded subsequences as follows:

$$S_0 \supset S_1 \supset \cdots \supset S_{j-1} \supset S_j \cdots. \tag{12}$$

For our later development, let us introduce some basic definitions concerning the inner product and the Kronecker symbol. Only real-valued functions are considered in this paper. The L^2-norm denotes the vector space, measurable square-integrable one-dimensional function. The inner product, denoted $\langle \cdot, \cdot \rangle$, of two real-valued functions $u(t) \in L^2$ and $v(t) \in L^2$ is then written as follows:

$$\langle u(t), v(t) \rangle = \int_{-\infty}^{+\infty} u(t) \times v(t) dt. \tag{13}$$

The Kronecker symbol, denoted $\delta_{p,q}$, is a function depending on two integer variables p and q. It is defined as follows:

$$\delta_{p,q} = \begin{cases} 1 & \text{if } p = q, \\ 0 & \text{if } p \neq q. \end{cases} \tag{14}$$

3.2. Orthonormal spline scaling basis on bounded intervals

The aim of this subsection is to explicitly construct the orthonormal spline basis of the spline scaling space. A multiresolution analysis consists in approximating a given signal $f(t)$, at different resolution levels j. These approximations are deduced from orthogonal projections of the signal on respective approximation subspaces. These subspaces are known as scaling or approximation subspaces. In this paper, the approximation subspace denoted V_j is spanned by the orthonormal spline basis functions of degree d defined on each bounded interval $I_{j,i}$ as follows:

$$V_j = \text{span}\,\{\varphi^d_{j,k,I_{j,i}}(t) = \underline{B}^d_{k,I_{j,i}}(t)\ \forall k \in [0,d];\ \forall i \in N\}. \tag{15}$$

The previously defined subsequences structure, given by (12), imposes therefore imbrications of the scaling subspaces as follows:

$$V_0 \supset V_1 \supset \cdots \supset V_{j-1} \supset V_j \cdots. \tag{16}$$

On each interval $I_{j,i}$, the scaling functions form obviously an orthonormal spline basis as explained in Section 2. Since the basis are defined on disjoint supports, the set of scaling functions $\{\varphi^d_{j,k,I_{j,i}}(t)$, for all $k \in [0,d]$; for all $i \in N\}$ at resolution j, is an orthonormal spline basis of the approximation subspace V_j, whatever the degree d of the spline function. So the scaling functions belonging to the subspace V_j satisfy the summarized orthonormal conditions, whatever the degree of the spline function:

$$\langle \varphi^d_{j,k,I_{j,i}}(t), \varphi^d_{j,l,I_{j,p}}(t) \rangle = \delta_{kl}\delta_{ip} \quad \text{for } k = 0,\ldots,d,\ l = 0,\ldots,d,\ i \in N,\ p \in N, \tag{17}$$

where $\langle \cdot, \cdot \rangle$ is the inner product of the two real functions $\varphi^d_{j,k,I_{j,i}}(t)$ and $\varphi^d_{j,l,I_{j,p}}(t)$ given by (13). δ_{kl} and δ_{ip} are the Kronecker symbols previously defined by (14).

As examples, we present the orthonormal spline basis spanning the basic spline scaling space V_0 for three degrees

of the spline function $d = 0$, $d = 1$, and $d = 2$. We start by providing the expression of the simplest case corresponding to the smallest spline function degree (i.e., $d = 0$). The scaling basis associated to the uniform spline function of degree $d = 0$ has been initially proposed by Haar. We suggest keeping the same appellation even in the irregular spaced knots. On each bounded interval $I_{0,i} \in S_0$, the basic spline space V_0 is spanned by the following scaling function:

$$\begin{aligned}\varphi^0_{0,0,I_{0,i}}(t) &= \underline{B}^0_{0,[t_i,t_{i+1}]}(t) \\ &= \frac{1}{\sqrt{t_{i+1}-t_i}} \quad \text{for } t \in I_{0,i}, \text{ and all } i \in N.\end{aligned} \tag{18}$$

We concentrate now on the construction of linear orthonormal spline scaling basis. Among the different construction possibilities inherent to the Gram-Schmidt method, we present the example built with the first nonuniform B-spline function as the reference component. At any given interval $I_{0,i}$, the expressions of the two linear spline scaling functions $\varphi^1_{0,k,I_{0,i}}(t) \in V_0$ are given below:

$$\begin{aligned}\varphi^1_{0,0,I_{0,i}}(t) &= \sqrt{3}\frac{t_{i+1}-t}{(t_{i+1}-t_i)^{3/2}}, \\ \varphi^1_{0,1,I_{0,i}}(t) &= \frac{3t-t_{i+1}-2t_i}{(t_{i+1}-t_i)^{3/2}} \quad \text{for } t \in I_{0,i} \text{ and all } i \in N.\end{aligned} \tag{19}$$

This last example concerns the quadratic orthonormal spline scaling basis of the basic space V_0. According to the Gram-Schmidt method, various quadratic orthonormal spline bases are possible. We present one construction among others. The quadratic spline scaling functions spanning the basic spline space V_0 are given as follows:

$$\begin{aligned}\varphi^2_{0,0,I_{0,i}}(t) &= \frac{\sqrt{5}(t_{i+1}-t)^2}{(t_{i+1}-t_i)^{5/2}}, \\ \varphi^2_{0,1,I_{0,i}}(t) &= \frac{\sqrt{3}(t_{i+1}-t)(5t-4t_i-t_{i+1})}{(t_{i+1}-t_i)^{5/2}}, \\ \varphi^2_{0,2,I_{0,i}}(t) &= \frac{(10t^2-(12t_i+8t_{i+1})t+3t_i^2+t_{i+1}^2+6t_it_{i+1})}{(t_{i+1}-t_i)^{5/2}} \\ &\qquad \text{for } t \in I_{0,i} \text{ and all } i \in N.\end{aligned} \tag{20}$$

The orthonormal spline scaling bases given by (18), (19), and (20) are plotted in Figure 1 on the interval $[0, 2]$.

3.3. Two-scale equation on irregular partition of knots

In the multiresolution traditional case, the two-scale equation plays a significant role in the design of fast orthogonal decomposition and reconstruction algorithms. This subsection shows that even if the partition of knots is irregular, it is possible again to obtain relationship between the spline scaling functions at resolution level j and $j-1$.

The approximation spline subspace V_{j-1} contains the subspace V_j (see (16)). So, any scaling function belonging to V_j, and defined on the sequence S_j, can be decomposed

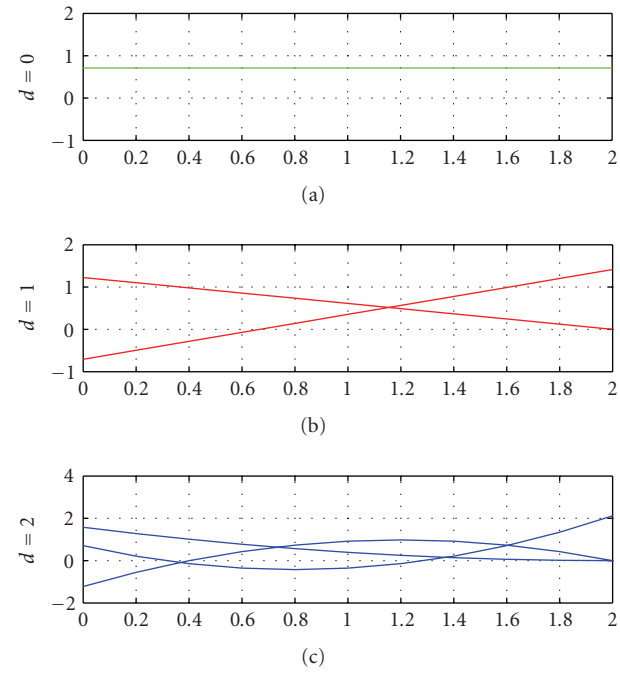

Figure 1: Orthonormal spline bases for $d = 0$, $d = 1$, and $d = 2$.

on each bounded interval $I_{j,i}$ using the basis of the approximation subspace V_{j-1} as follows:

$$\varphi^d_{j,k,I_{j,i}}(t) = \sum_{m=0}^{1}\sum_{n=0}^{d} h^{m,n}_{j,k}\left(t_{2^{j-1}i}, t_{2^{j-1}(i+1)}, t_{2^{j-1}(i+2)}\right)\varphi^d_{j-1,n,I_{j-1,i+m}}(t) \quad \text{for } t \in I_{j,i},\ k \in [0,d],\ i \in N, \tag{21}$$

where $h^{m,n}_{j,k}$ represent weighted coefficients which will be computed later.

Since $\langle \varphi^d_{j,k,I_{j,i}}(t), \varphi^d_{j,l,I_{j,p}}(t)\rangle = \delta_{kl}\delta_{ip}$ (for all $k \in [0,d]$, for all $l \in [0,d]$, for all $i \in N$ and for all $p \in N$), it is easy to show, after some manipulations, that the weighted coefficients are deduced by these equations

$$h^{m,n}_{j,k}\left(t_{2^{j-1}i}, t_{2^{j-1}(i+1)}, t_{2^{j-1}(i+2)}\right) = \left\langle \varphi^d_{j,k,I_{j,i}}(t), \varphi^d_{j-1,n,I_{j-1,i+m}}(t)\right\rangle, \quad \forall k \in [0,d],\ n = [0,d],\ m = 0,1,\ i \in N. \tag{22}$$

In irregular knots partition, (22) proves that the filter coefficients are parameterized by the positions of the knots belonging to the sequence S_{j-1}. For writing convenience reasons, these coefficients are gathered in a matrix, denoted $\mathbf{H}_j(t_{2^{j-1}i}, t_{2^{j-1}(i+1)}, t_{2^{j-1}(i+2)})$ of dimension $(d+1)\times 2(d+1)$, as follows:

$$\mathbf{H}_j\left(t_{2^{j-1}i}, t_{2^{j-1}(i+1)}, t_{2^{j-1}(i+2)}\right) = \begin{pmatrix} h^{0,0}_{j,0} & \cdots & h^{0,d}_{j,0} & h^{1,0}_{j,0} & \cdots & h^{1,d}_{j,0} \\ \vdots & & \vdots & \vdots & & \vdots \\ h^{0,0}_{j,d} & \cdots & h^{0,d}_{j,d} & h^{1,0}_{j,d} & \cdots & h^{1,d}_{j,d} \end{pmatrix}. \tag{23}$$

These results show that the standard filter banks are replaced by a set of filters depending on the position of the knots in the sequence.

To illustrate these results, we provide the explicit expressions of the filter coefficients for three different degrees $d = 0$, $d = 1$, and $d = 2$. The approximation spline space V_0 contains the subspace V_1 ($V_1 \subset V_0$). So, any scaling function belonging to V_1, and defined on any bounded interval $I_{1,i} \in S_1$, can be decomposed using the basis of the approximation space V_0. We start by the simplest case, that is, $d = 0$. The Haar scaling function $\varphi^0_{1,0,I_{1,i}}(t)$ is thus decomposed as follows:

$$\varphi^0_{1,0,I_{1,i}}(t) = h^{0,0}_{1,0}(t_i, t_{i+1}, t_{i+2})\varphi^0_{0,0,I_{0,i}}(t) + h^{1,0}_{1,0}(t_i, t_{i+1}, t_{i+2})\varphi^0_{0,0,I_{0,i+1}}(t) \quad \text{for } t \in I_{1,i},\ i \in N. \tag{24}$$

The weighted coefficients $\{h^{0,0}_{1,0}(t_i, t_{i+1}, t_{i+2}), h^{1,0}_{1,0}(t_i, t_{i+1}, t_{i+2})\}$, computed as explained below, provides the following solutions:

$$h^{0,0}_{1,0}(t_i, t_{i+1}, t_{i+2}) = \frac{\sqrt{t_{i+1} - t_i}}{\sqrt{t_{i+2} - t_i}},$$
$$h^{1,0}_{1,0}(t_i, t_{i+1}, t_{i+2}) = \frac{\sqrt{t_{i+2} - t_{i+1}}}{\sqrt{t_{i+2} - t_i}} \quad \forall i \in N. \tag{25}$$

Consider now the linear spline scaling case. The decomposition of any linear spline scaling function $\{\varphi^1_{1,0,I_{1,i}}(t), \varphi^1_{1,1,I_{1,i}}(t)\} \in V_1$, on the basic space V_0 is expressed as a linear combination of weighted coefficients by scaling functions $\{\varphi^1_{0,0,I_{0,i}}(t), \varphi^1_{0,1,I_{0,i}}(t), \varphi^1_{0,0,I_{0,i+1}}(t), \varphi^1_{0,1,I_{0,i+1}}(t)\} \in V_0$ as follows:

$$\begin{aligned}\varphi^1_{1,0I_{1,i}}(t) &= h^{0,0}_{1,0}(t_i, t_{i+1}, t_{i+2})\varphi^1_{0,0,I_{0,i}}(t) + h^{0,1}_{1,0}(t_i, t_{i+1}, t_{i+2})\varphi^1_{0,1,I_{0,i}}(t) \\ &\quad + h^{1,0}_{1,0}(t_i, t_{i+1}, t_{i+2})\varphi^1_{0,0,I_{0,i+1}}(t) + h^{1,1}_{1,0}(t_i, t_{i+1}, t_{i+2})\varphi^1_{0,1,I_{0,i+1}}(t),\end{aligned} \tag{26}$$

$$\begin{aligned}\varphi^1_{1,1,I_{1,i}}(t) &= h^{0,0}_{1,1}(t_i, t_{i+1}, t_{i+2})\varphi^1_{0,0,I_{0,i}}(t) + h^{0,1}_{1,1}(t_i, t_{i+1}, t_{i+2})\varphi^1_{0,1,I_{0,i}}(t) \\ &\quad + h^{1,0}_{1,1}(t_i, t_{i+1}, t_{i+2})\varphi^1_{0,0,I_{0,i+1}}(t) + h^{1,1}_{1,1}(t_i, t_{i+1}, t_{i+2})\varphi^1_{0,1,I_{0,i+1}}(t).\end{aligned} \tag{27}$$

After some appropriate manipulations (see (22)), we obtain the following expressions for each filter coefficients:

$$h^{0,0}_{1,0}(t_i, t_{i+1}, t_{i+2}) = \frac{(1/2)(t_{i+1} - t_i)^{1/2}(3t_{i+2} - 2t_i - t_{i+1})}{(t_{i+2} - t_i)^{3/2}};$$
$$h^{0,1}_{1,0}(t_i, t_{i+1}, t_{i+2}) = \frac{(\sqrt{3}/2)(t_{i+1} - t_i)^{1/2}(t_{i+2} - t_{i+1})}{(t_{i+2} - t_i)^{3/2}};$$
$$h^{1,0}_{1,0}(t_i, t_{i+1}, t_{i+2}) = \frac{(t_{i+2} - t_{i+1})^{3/2}}{(t_{i+2} - t_i)^{3/2}};$$
$$h^{1,1}_{1,0}(t_i, t_{i+1}, t_{i+2}) = 0;$$
$$h^{0,0}_{1,1}(t_i, t_{i+1}, t_{i+2}) = \frac{-(\sqrt{3}/2)(t_{i+1} - t_i)^{1/2}(t_{i+2} - t_{i+1})}{(t_{i+2} - t_i)^{3/2}};$$
$$h^{0,1}_{1,1}(t_i, t_{i+1}, t_{i+2}) = \frac{-(1/2)(t_{i+1} - t_i)^{1/2}(t_{i+2} + 2t_i - 3t_{i+1})}{(t_{i+2} - t_i)^{3/2}};$$
$$h^{1,0}_{1,1}(t_i, t_{i+1}, t_{i+2}) = \frac{\sqrt{3}(t_{i+1} - t_i)(t_{i+2} - t_{i+1})^{1/2}}{(t_{i+2} - t_i)^{3/2}};$$
$$h^{1,1}_{1,1}(t_i, t_{i+1}, t_{i+2}) = \frac{\sqrt{t_{i+2} - t_{i+1}}}{\sqrt{t_{i+2} - t_i}} \quad \forall i \in N. \tag{28}$$

It was shown that the more spline function degree increases, the better the approximation quality of the signal is [12]. For this reason, we are interested in high degrees although the number of weighted coefficients to determine becomes significant. The weighted coefficients of the quadratic spline scaling functions $\{\varphi^2_{1,0,I_{1,i}}(t), \varphi^2_{1,1,I_{1,i}}(t), \varphi^2_{1,2,I_{1,i}}(t)\} \in V_1$ are presented at the following:

$$h^{0,0}_{1,0}(t_i, t_{i+1}, t_{i+2}) = \frac{(t_{i+1} - t_i)^{1/2}(6t_i^2 + 3t_i t_{i+1} - 15t_i t_{i+2} + t_{i+1}^2 - 5t_{i+1}t_{i+2} + 10t_{i+2}^2)}{6(t_{i+2} - t_i)^{5/2}};$$
$$h^{1,1}_{1,0}(t_i, t_{i+1}, t_{i+2}) = 0;$$
$$h^{0,1}_{1,0}(t_i, t_{i+1}, t_{i+2}) = \sqrt{15}\frac{(t_{i+1} - t_i)^{1/2}(t_{i+2} - t_{i+1})(2t_{i+2} - t_{i+1} - t_i)}{6(t_{i+2} - t_i)^{5/2}};$$
$$h^{0,2}_{1,0}(t_i, t_{i+1}, t_{i+2}) = \frac{\sqrt{5}(t_{i+1} - t_i)^{1/2}(t_{i+2} - t_{i+1})}{3(t_{i+2} - t_i)^{5/2}};$$
$$h^{1,0}_{1,0}(t_i, t_{i+1}, t_{i+2}) = \frac{(t_{i+2} - t_{i+1})^{5/2}}{(t_{i+2} - t_i)^{5/2}};$$
$$h^{1,2}_{1,0}(t_i, t_{i+1}, t_{i+2}) = 0;$$
$$h^{0,0}_{1,1}(t_i, t_{i+1}, t_{i+2}) = \frac{\sqrt{15}}{6}\frac{(t_{i+1} - t_i)^{1/2}(t_{i+2} - t_{i+1})(t_i + t_{i+1} - 2t_{i+2})}{(t_{i+2} - t_i)^{5/2}};$$
$$h^{0,1}_{1,1}(t_i, t_{i+1}, t_{i+2}) = \frac{(t_{i+1} - t_i)^{1/2}(2t_i^2 - 2t_{i+2}^2 + 9t_{i+1}t_{i+2} - 5t_{i+1}^2 - 5t_i t_{i+2} + t_i t_{i+1})}{2(t_{i+2} - t_i)^{5/2}};$$
$$h^{0,0}_{1,2}(t_i, t_{i+1}, t_{i+2}) = \frac{\sqrt{5}(t_{i+2} - t_{i+1})^2(t_{i+1} - t_i)^{1/2}}{3(t_{i+2} - t_i)^{5/2}};$$
$$h^{0,2}_{1,1}(t_i, t_{i+1}, t_{i+2}) = \frac{\sqrt{3}}{3}\frac{(t_{i+1} - t_i)^{1/2}(t_{i+2} - t_{i+1})(5t_{i+1} - t_{i+2} - 4t_i)}{(t_{i+2} - t_i)^{5/2}};$$
$$h^{1,0}_{1,1}(t_i, t_{i+1}, t_{i+2}) = \frac{-\sqrt{15}(t_{i+2} - t_{i+1})^{3/2}(t_i - t_{i+1})}{(t_{i+2} - t_i)^{5/2}};$$
$$h^{1,1}_{1,1}(t_i, t_{i+1}, t_{i+2}) = \frac{(t_{i+2} - t_{i+1})^{3/2}}{(t_{i+2} - t_i)^{3/2}};$$
$$h^{1,2}_{1,1}(t_i, t_{i+1}, t_{i+2}) = 0;$$

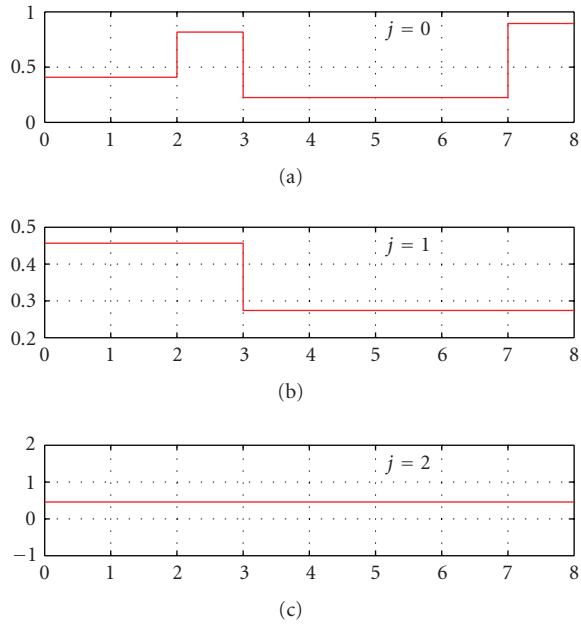

Figure 2: Haar scaling functions at resolutions $j = 0, 1, 2$.

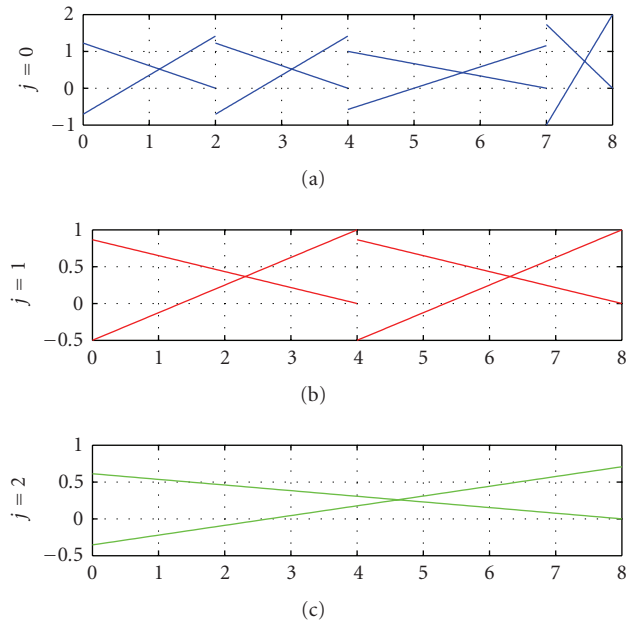

Figure 3: Linear scaling functions at resolutions $j = 0, 1, 2$.

$$
\begin{aligned}
&h_{1,2}^{0,1}(t_i, t_{i+1}, t_{i+2}) \\
&\quad = \frac{\sqrt{3}}{3}\frac{(t_{i+2}-t_{i+1})(t_{i+1}-t_i)^{1/2}(t_{i+2}+4t_i-5t_{i+1})}{(t_{i+2}-t_i)^{5/2}};\\
&h_{1,2}^{0,2}(t_i, t_{i+1}, t_{i+2}) \\
&\quad = \frac{(t_{i+1}-t_i)^{1/2}(3t_i^2-12t_it_{i+1}+6t_{i+2}t_i+t_{i+2}^2+10t_{i+1}^2-8t_{i+2}t_{i+1})}{3(t_{i+2}-t_i)^{5/2}};\\
&h_{1,2}^{1,1}(t_i, t_{i+1}, t_{i+2}) = \sqrt{3}\frac{(t_{i+1}-t_i)(t_{i+2}-t_{i+1})^{1/2}}{(t_{i+2}-t_i)^{3/2}};\\
&h_{1,2}^{1,0}(t_i, t_{i+1}, t_{i+2}) \\
&\quad = \sqrt{5}\frac{(t_i-t_{i+1})(t_{i+2}-t_{i+1})^{1/2}(t_{i+2}-2t_{i+1}+t_i)}{(t_{i+2}-t_i)^{5/2}};\\
&h_{1,2}^{1,2}(t_i, t_{i+1}, t_{i+2}) = \frac{(t_{i+2}-t_{i+1})^{1/2}}{(t_{i+2}-t_i)^{1/2}} \quad \forall i \in N.
\end{aligned}
\tag{29}
$$

The relationships between other successive resolutions are directly derived from the preceding solutions specified for the resolution level $j = 1$. These solutions show clearly that the filter coefficients depend on the localization of the sequence knots.

Figures 2, 3, and 4 present, respectively, Haar, linear, and quadratic spline scaling functions at three resolution levels $j = 0, 1, 2$ starting on the initial finest non-equally spaced knots sequence $S_0 = [t_0 = 0, t_1 = 2, t_2 = 4, t_3 = 7, t_4 = 8]$.

4. SPLINE WAVELET FUNCTION ON IRREGULAR PARTITION OF KNOTS

This section is devoted to the construction of orthonormal spline wavelet bases using the multiresolution specific requirements in the context of irregular partition of knots. We begin the study by introducing the subspaces where the spline wavelet functions live.

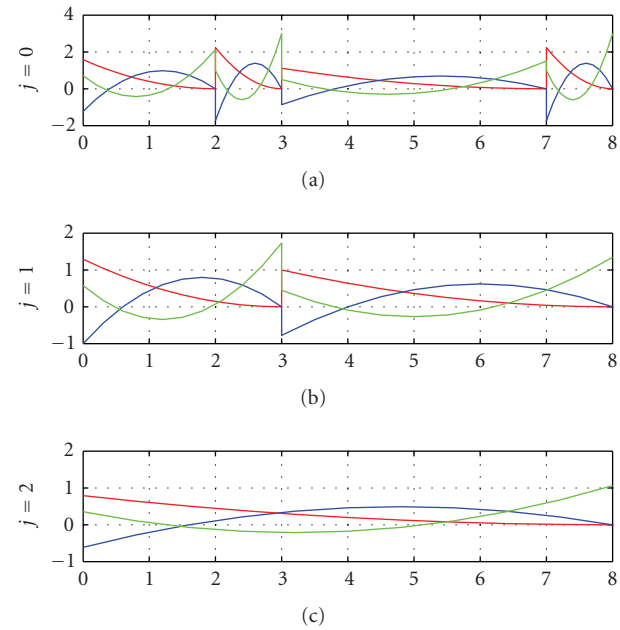

Figure 4: Quadratic scaling functions at resolutions $j = 0, 1, 2$.

4.1. Spline detail subspaces

The successive approximations of a signal at two successive resolutions $j-1$ and j are, respectively, obtained from the orthogonal projections of this signal on the respective approximation subspaces V_{j-1} and V_j. The embedded structure of

the spline scaling subspaces involves the inclusion of the subspace V_j in V_{j-1}. To improve the approximated signal quality, at resolution j, one classically introduces the orthogonal complement of V_j in V_{j-1}. This orthogonal subspace, known as detail subspace, is denoted W_j. Hence, the mathematical relationship between these subspaces is as follows:

$$V_{j-1} = V_j \oplus W_j, \tag{30}$$

where the symbol $\oplus$ represents the direct sum between the approximation and detail subspaces V_j and W_j.

This detail subspace is spanned from a set of wavelet functions denoted $\psi^d_{j,k,I_{j,i}}(t)$. The dimension of the wavelet space, on any bounded interval $I_{j,i} = I_{j-1,i} \cup I_{j-1,i+1}$, is deduced from the previous relation as follows:

$$\dim(W_j) = \dim(V_{j-1}) - \dim(V_j) \quad \forall j \geq 1, \tag{31}$$

where $\dim(V_{j-1}) = 2 \times (d+1)$ and $\dim(V_j) = d+1$.

The dimension of the spline wavelet subspace is thus easily deduced and is equal to

$$\dim(W_j) = d+1 \quad \forall j \geq 1. \tag{32}$$

Therefore, the detail subspace W_j is spanned by the spline wavelet functions defined on each bounded interval $I_{j,i}$ as follows:

$$W_j = \operatorname{span}\{\psi^d_{j,k,I_{j,i}}(t)\ \forall k \in [0,d];\ \forall j \geq 1;\ \forall i \in N\}. \tag{33}$$

4.2. Two-scale equation on irregular partition of knots

According to (30), the wavelet subspace W_j is contained in the approximation subspace V_{j-1}. Thus, the kth wavelet function $\psi^d_{j,k,I_{j,i}}(t)$, at resolution level j, can be expressed as a linear combination of coefficients $\{g^{m,n}_{j,k}\}$ weighted by scaling functions belonging to the spline subspace V_{j-1}. Therefore, on each interval $I_{j,i} = I_{j-1,i} \cup I_{j-1,i+1}$, we obtain the following decomposition refereeing to the two-scale equation:

$$\psi^d_{j,k,I_{j,i}}(t) = \sum_{m=0}^{1}\sum_{n=0}^{d} g^{m,n}_{j,k}\left(t_{2^{j-1}i}, t_{2^{j-1}(i+1)}, t_{2^{j-1}(i+2)}\right)\varphi^d_{j-1,n,I_{j-1,i+m}}(t)$$
$$\text{with } k = 0,\ldots,d,\ m = 0,1,\ n = 0,\ldots,d,\ i \in N. \tag{34}$$

For writing convenience reasons, the weighted coefficients are also gathered in a matrix, denoted $\mathbf{G}_j(t_{2^{j-1}i}, t_{2^{j-1}(i+1)}, t_{2^{j-1}(i+2)})$ of dimension $(d+1) \times 2(d+1)$, as follows:

$$\mathbf{G}_j\left(t_{2^{j-1}i}, t_{2^{j-1}(i+1)}, t_{2^{j-1}(i+2)}\right) = \begin{pmatrix} g^{0,0}_{j,0} & \cdots & g^{0,d}_{j,0} & g^{1,0}_{j,0} & \cdots & g^{1,d}_{j,0} \\ \vdots & & \vdots & \vdots & & \vdots \\ g^{0,0}_{j,d} & \cdots & g^{0,d}_{j,d} & g^{1,0}_{j,d} & \cdots & g^{1,d}_{j,d} \end{pmatrix}. \tag{35}$$

The spline wavelet function requires the computation of the two-scale equation coefficients $\{g^{m,n}_{j,k}\}$. To compute these $2(d+1)^2$ coefficients, one must satisfy the conditions inherent to the traditional multiresolution concept listed below.

(i) The spline scaling subspace is orthogonal to the wavelet subspace, for any resolution level ($j \geq 1$) resulting in

$$\left\langle \psi^d_{j,k,I_{j,i}}(t), \varphi^d_{j,l,I_{j,p}}(t) \right\rangle = 0 \quad \text{with } \forall k \in [0,d],\ \forall l \in [0,d],\ \forall i \in N,\ \forall p \in N. \tag{36}$$

(ii) The orthonormality conditions of the wavelet basis at all and cross resolution levels resulting in

$$\left\langle \psi^d_{j,k,I_{j,i}}(t), \psi^d_{j,l,I_{j,p}}(t) \right\rangle = \delta_{kl}\delta_{ip} \quad \text{with } \forall k \in [0,d],\ \forall l \in [0,d],\ \forall i \in N,\ \forall p \in N. \tag{37}$$

These conditions gathered lead to solve the following system of equations:

$$\mathbf{H}_j\left(t_{2^{j-1}i}, t_{2^{j-1}(i+1)}, t_{2^{j-1}(i+2)}\right)\mathbf{G}_j\left(t_{2^{j-1}i}, t_{2^{j-1}(i+1)}, t_{2^{j-1}(i+2)}\right)^t = \mathbf{0},$$
$$\mathbf{G}_j\left(t_{2^{j-1}i}, t_{2^{j-1}(i+1)}, t_{2^{j-1}(i+2)}\right)\mathbf{G}_j\left(t_{2^{j-1}i}, t_{2^{j-1}(i+1)}, t_{2^{j-1}(i+2)}\right)^t = \mathbf{I}_d. \tag{38}$$

To find the $2(d+1)^2$ unknown coefficients $\{g^{m,n}_{j,k}\}$, we must find the basis of the $\mathbf{H}_j(t_{2^{j-1}i}, t_{2^{j-1}(i+1)}, t_{2^{j-1}(i+2)})$ null space. The system of (38) has $d(d+1)/2$ freedom degrees. Many solutions are possible involving then the construction of a large family of orthonormal wavelet bases. The freedom degrees can be used judiciously to ensure some desirable features of the wavelet functions. The system of (38) shows that the standard filter banks are replaced by a set of filters depending on the position of the knots in the sequence. Some examples will be provided later.

4.3. Orthonormal spline wavelet basis on bounded intervals

According to the theoretical development of the spline wavelet bases on the irregular partition context of knots, we provide explicit expressions of the wavelet bases for three degrees $d = 0$, $d = 1$, and $d = 2$ in order to complete the required tools of a multiresolution analysis since the scaling bases have been already built in Section 3.

The Haar wavelet is firstly presented. Due to the structure of the multiresolution subspaces, the wavelet functions $\{\psi^0_{1,0,I_{1,i}}(t)\}$ belonging to W_1, can be expressed, on each bounded interval $I_{1,i} = I_{0,i} \cup I_{0,i+1}$, as follows:

$$\psi^0_{1,0,I_{1,i}}(t) = g^{0,0}_{1,0}(t_i, t_{i+1}, t_{i+2})\varphi^0_{0,0,I_{0,i}}(t) + g^{1,0}_{1,0}(t_i, t_{i+1}, t_{i+2})\varphi^0_{0,0,I_{0,i+1}}(t). \tag{39}$$

The two weighted coefficients $g^{0,0}_{1,0}(t_i, t_{i+1}, t_{i+2})$, $g^{1,0}_{1,0}(t_i, t_{i+1}, t_{i+2})$ are computed as previously explained. Replacing the scaling functions by their explicit expressions, given by (19), the generalized system of (38) becomes

$$\begin{aligned} &(t_{i+1} - t_i)g^{0,0}_{1,0}(t_i, t_{i+1}, t_{i+2}) \\ &\quad + (t_{i+2} - t_{i+1})g^{1,0}_{1,0}(t_i, t_{i+1}, t_{i+2}) = 0, \\ &(t_{i+1} - t_i)\left(g^{0,0}_{1,0}(t_i, t_{i+1}, t_{i+2})\right)^2 \\ &\quad + (t_{i+2} - t_{i+1})\left(g^{1,0}_{1,0}(t_i, t_{i+1}, t_{i+2})\right)^2 = 1. \end{aligned} \tag{40}$$

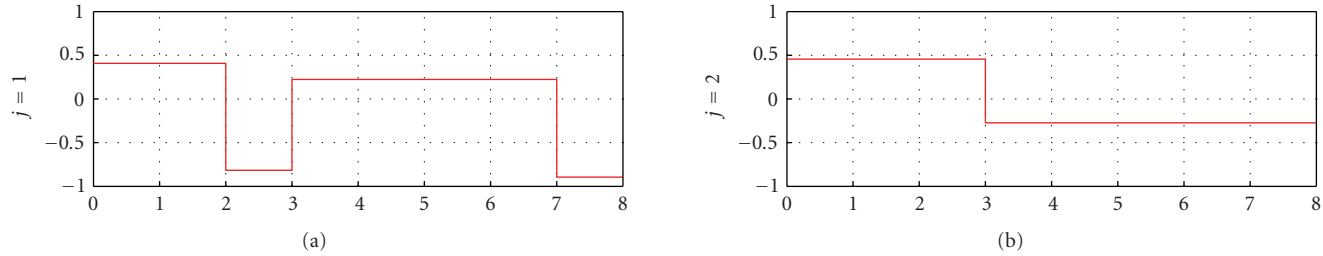

Figure 5: Haar wavelet functions at resolution levels $j = 1, 2$.

Two distinct solutions are found:

$$g_{1,0}^{0,0}(t_i, t_{i+1}, t_{i+2}) = \pm\frac{\sqrt{t_{i+2} - t_{i+1}}}{\sqrt{t_{i+2} - t_i}} \quad \text{for } t_i \le t < t_{i+1},$$
$$g_{1,0}^{1,0}(t_i, t_{i+1}, t_{i+2}) = \mp\frac{\sqrt{t_{i+1} - t_i}}{\sqrt{t_{i+2} - t_i}} \quad \text{for } t_{i+1} \le t < t_{i+2}. \tag{41}$$

The relationships between successive resolutions are easily deduced from the above equations. Figure 5 presents, at two resolution levels $j = 1, 2$, the Haar wavelet function using one provided solution given by (41) on the finest sequence $S_0 = [t_0 = 0, t_1 = 2, t_2 = 4, t_3 = 7, t_4 = 8]$. The first graph, concerns the two wavelets functions $\{\psi_{1,0,[0,3]}^0(t), \psi_{1,1,[3,8]}^0(t)\}$ generating the space W_1. The second graph represents the wavelet function $\psi_{2,0,[0,8]}^0(t)$ spanning the space W_2.

According to the theoretical development, the linear spline wavelet functions $\{\psi_{1,k,I_{1,i}}^1(t)$, for $k = 0, 1\}$ can be decomposed using the previous linear scaling basis of the space V_0 previously constructed (20) as follows:

$$\begin{aligned}
\psi_{1,0,I_{1,i}}^1(t) &= g_{1,0}^{0,0}(t_i, t_{i+1}, t_{i+2})\varphi_{0,0,I_{0,i}}^1(t) \\
&\quad + g_{1,0}^{0,1}(t_i, t_{i+1}, t_{i+2})\varphi_{0,1,I_{0,i}}^1(t) \\
&\quad + g_{1,0}^{1,0}(t_i, t_{i+1}, t_{i+2})\varphi_{0,0,I_{0,i+1}}^1(t) \\
&\quad + g_{1,0}^{1,1}(t_i, t_{i+1}, t_{i+2})\varphi_{0,1,I_{0,i+1}}^1, \\
\psi_{1,1,I_{1,i}}^1(t) &= g_{1,1}^{0,0}(t_i, t_{i+1}, t_{i+2})\varphi_{0,0,I_{0,i}}^1(t) \\
&\quad + g_{1,1}^{0,1}(t_i, t_{i+1}, t_{i+2})\varphi_{0,1,I_{0,i}}^1(t) \\
&\quad + g_{1,1}^{1,0}(t_i, t_{i+1}, t_{i+2})\varphi_{0,0,I_{0,i+1}}^1(t) \\
&\quad + g_{1,1}^{1,1}(t_i, t_{i+1}, t_{i+2})\varphi_{0,1,I_{0,i+1}}^1(t).
\end{aligned} \tag{42}$$

The linear wavelet basis construction requires the computation of eight unknown coefficients $\{g_{1,k}^{m,n}(t_i, t_{i+1}, t_{i+2})\}$. These coefficients are obtained by solving the equation system (38). In the linear case, only one freedom degree is available. This freedom degree can be used judiciously in order to impose continuity condition of at least one wavelet function on each knot $t_{2^{j-1}(i+1)}$ inside the interval $I_{j,i}$. For this particular case, explicit expressions of the coefficients $\{g_{1,k}^{m,n}(t_i, t_{i+1}, t_{i+2})\}$ are listed below:

$$\begin{aligned}
g_{1,0}^{0,0}(t_i, t_{i+1}, t_{i+2}) &= 0; \\
g_{1,0}^{0,1}(t_i, t_{i+1}, t_{i+2}) &= \frac{\sqrt{t_{i+2} - t_{i+1}}}{\sqrt{t_{i+2} - t_i}}; \\
g_{1,0}^{1,0}(t_i, t_{i+1}, t_{i+2}) &= -(\sqrt{3}/2)\frac{\sqrt{t_{i+1} - t_i}}{\sqrt{t_{i+2} - t_i}}; \\
g_{1,0}^{1,1}(t_i, t_{i+1}, t_{i+2}) &= (1/2)\frac{\sqrt{t_{i+1} - t_i}}{\sqrt{t_{i+2} - t_i}}; \\
g_{1,1}^{0,0}(t_i, t_{i+1}, t_{i+2}) &= \frac{(t_{i+2} - t_{i+1})^{3/2}}{(t_{i+2} - t_i)^{3/2}}; \\
g_{1,1}^{0,1}(t_i, t_{i+1}, t_{i+2}) &= -\frac{\sqrt{3}(t_{i+2} - t_{i+1})^{1/2}(t_{i+1} - t_i)}{(t_{i+2} - t_i)^{3/2}}; \\
g_{1,1}^{1,0}(t_i, t_{i+1}, t_{i+2}) &= \frac{(1/2)(t_{i+1} - t_i)^{1/2}(4t_{i+1} - 3t_{i+2} - t_i)}{(t_{i+2} - t_i)^{3/2}}; \\
g_{1,1}^{1,1}(t_i, t_{i+1}, t_{i+2}) &= \frac{(\sqrt{3}/2)\sqrt{t_{i+1} - t_i}}{\sqrt{t_{i+2} - t_i}}.
\end{aligned} \tag{43}$$

The relationships between successive resolutions are directly deduced from the above equations.

Figure 6 presents linear wavelet functions $\{\psi_{1,0,I_{1,0}}^1(t)$, $\psi_{1,1,I_{1,0}}^1(t)\}$ on the interval $[2, 5]$ at resolution level $j = 1$, according to four solutions (a), (b), (c), (d) depending on the freedom degree of the equation system (38). Among these solutions, the graphs (a) show that the continuity of one wavelet function $\psi_{1,1,I_{1,0}}^1(t)$ is ensured at the knot $t_1 = 3$. Figure 7 presents the linear wavelet bases at two resolution levels $j = 1, 2$ on the initial finest sequence $S_0 = [t_0 = 0, t_1 = 2, t_2 = 4, t_3 = 7, t_4 = 8]$.

The quadratic spline wavelet functions $\{\psi_{1,k,I_{1,i}}^2(t)$, for $k = 0, 1, 2\}$ can be decomposed using the basis of the approximation space V_0 as follows:

$$\begin{aligned}
&\psi_{1,k,I_{1,i}}^2(t) \\
&= \sum_{m=0}^{1}\sum_{n=0}^{2} g_{1,k}^{m,n}(t_i, t_{i+1}, t_{i+2})\varphi_{0,n,I_{0,i}}^2(t) \\
&\quad + \sum_{m=0}^{1}\sum_{n=0}^{2} g_{1,k}^{m,n}(t_i, t_{i+1}, t_{i+2})\varphi_{0,n,I_{0,i+1}}^2(t) \quad \text{for } k = 0, 1, 2.
\end{aligned} \tag{44}$$

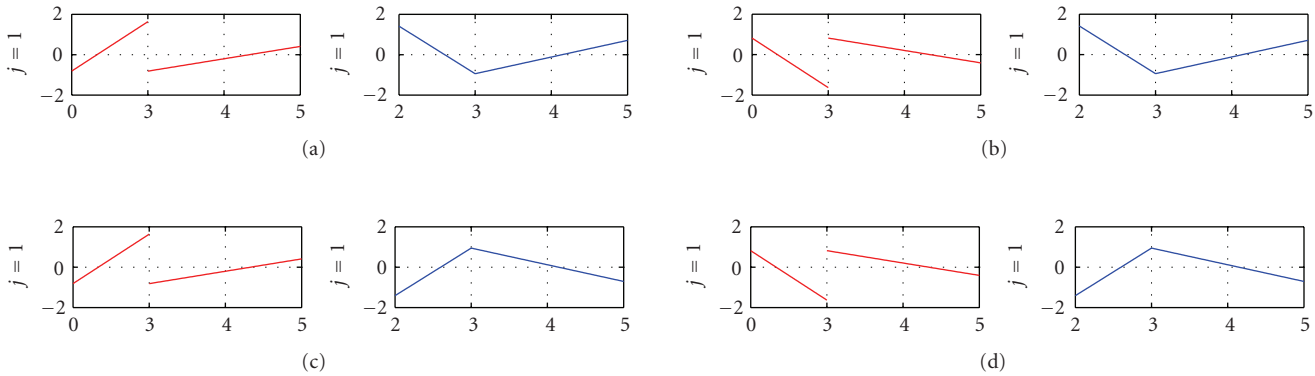

FIGURE 6: Four orthonormal linear wavelet bases at resolution level $j = 1$.

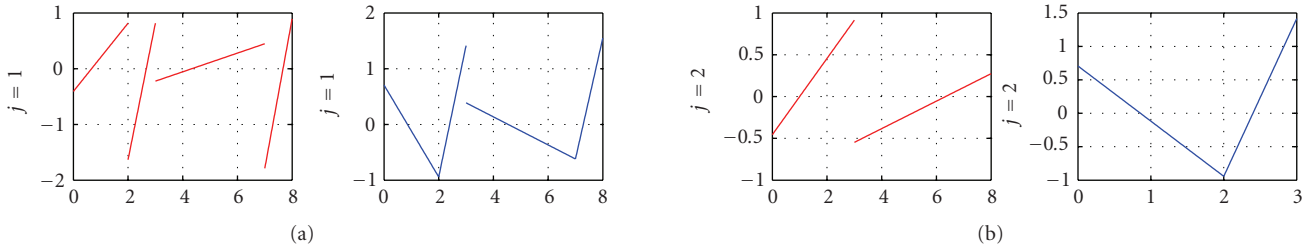

FIGURE 7: Linear wavelet functions at resolution levels $j = 1, 2$.

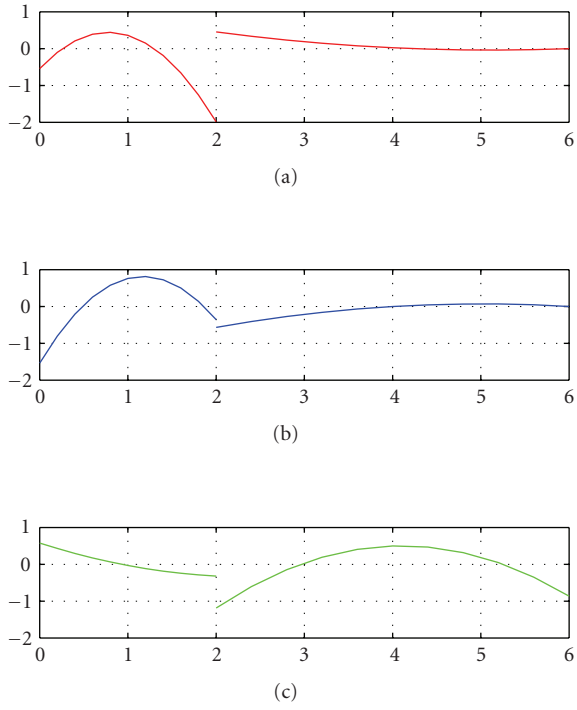

FIGURE 8: Orthonormal quadratic wavelet basis (no particular conditions).

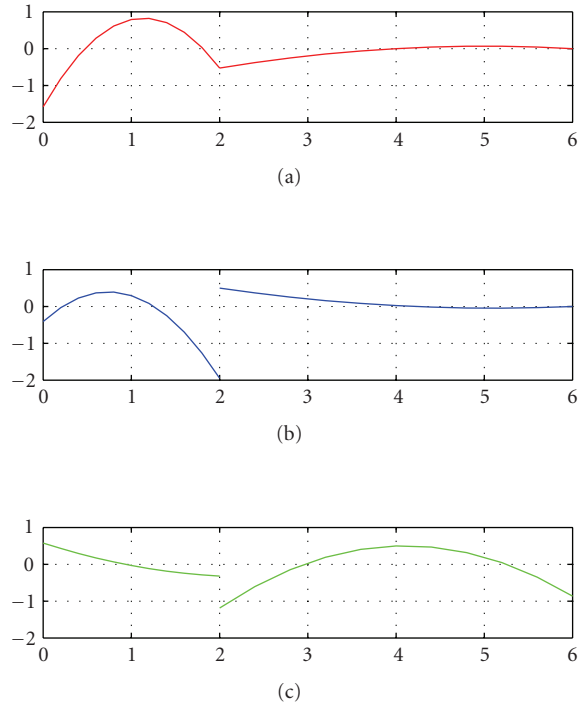

FIGURE 9: Orthonormal quadratic wavelet basis (one continuity condition).

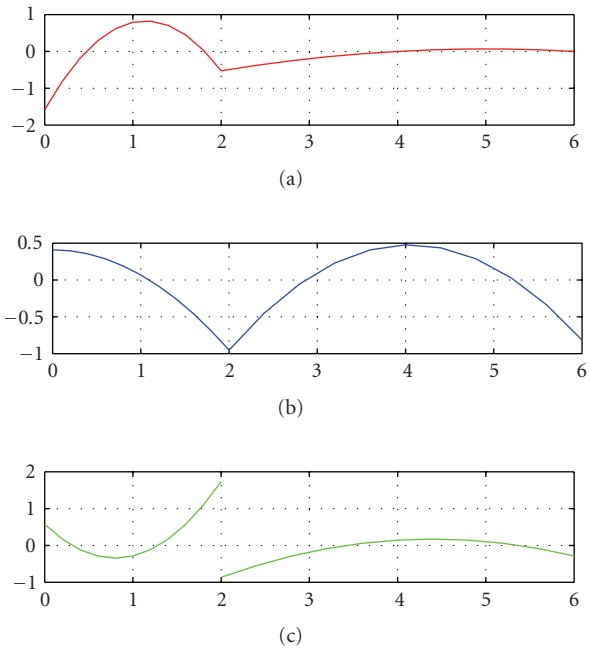

Figure 10: Orthonormal quadratic wavelet basis (two continuity conditions).

The 18 unknown coefficients $\{g_{1,k}^{m,n}(t_i, t_{i+1}, t_{i+2})$, for $m = 0, 1$; $n = 0, 1, 2$ and $k = 0, 1, 2\}$ are deduced from the resolution of the equation system (38) which has three freedom degrees. The graphs of Figure 8 present an example of orthonormal quadratic spline wavelet basis at resolution level $j = 1$ on the initial sequence $S_0 = [0, 2, 6]$. No particular condition is imposed to these wavelet functions while in Figure 9 only one freedom degree is exploited to ensure the continuity of the first wavelet function on the bounded interval $[0, 6]$, at the knot 2. Figure 10 uses two freedom degrees to ensure the continuity of the first and second wavelet functions.

5. ORTHOGONAL DECOMPOSITION AND RECONSTRUCTION

This section concerns the orthogonal decomposition of a given signal $f(t)$ using the scaling and wavelet functions presented in the previous section. At any resolution level $j-1$, the approximation of the signal $f(t)$ on the spline subspace V_{j-1} on the interval $I_{j-1,i}$, is denoted as $f_{j-1,I_{j-1,i}}(t)$. Starting with the orthogonally property of the scaling and wavelet subspaces ($V_{j-1} = V_j \oplus W_j$), one can decompose the signal $f_{j-1,I_{j-1,i}}(t) \in V_{j-1}$, on each interval $I_{j-1,i}$, according to the following relation:

$$f_{j-1,I_{j-1,i}}(t) = f_{j,I_{j,i}}(t) + r_{j,I_{j,i}}(t) \quad \text{for } i \in N,\ j > 1, \tag{45}$$

where $r_{j,I_{j,i}}(t)$ is the detail signal at resolution level j. Since the approximation signal $f_{j,I_{j,i}}(t)$ (resp., $r_{j,I_{j,i}}(t)$) belongs to V_j (resp., W_j) the function can be expressed as a linear weighted combination of the functions belonging to V_j (resp., W_j). Thus, the approximation of the signal $f_{j-1,I_{j-1,i}}(t) \in V_{j-1}$ becomes

$$\begin{aligned} f_{j-1,I_{j-1,i}}(t) = &\sum_{m=2i}^{2i+1} \sum_{k=0}^{1} c_{j,k}^{m} \varphi_{j,k,I_{j,m}}^{d}(t) \\ &+ \sum_{m=2i}^{2i+1} \sum_{k=0}^{1} d_{j,k}^{m} \psi_{j,k,I_{j,m}}^{d}(t) \quad \forall i \in N, \end{aligned} \tag{46}$$

where the weighted coefficients $\{c_{j,k}^{m}\}$ (resp., $\{d_{j,k}^{m}\}$) are given by the orthogonal projection of $f_{j,I_{j,i}}(t)$ (resp., $r_{j,I_{j,i}}(t)$) on the approximation subspace V_j (resp., W_j). After some manipulations, we show that these coefficients $\{c_{j,k}^{m}\}$ are closely related to $\{c_{j-1,k}^{l}\}$ and $\{h_{j,k}^{l,n}\}$, on the bounded interval $I_{j,i}$, as follows:

$$c_{j,k}^{m} = \sum_{l=2i}^{2i+1} \sum_{n=0}^{1} h_{j,k}^{l,n} c_{j-1,k}^{l} \quad \text{for } k = 0, 1;\ m = 2i, 2i+1; \text{ and all } i \in N. \tag{47}$$

This expression can be written in a matrix form as follows:

$$\underline{\mathbf{c}}_{j,I_{j,i}} = \mathbf{H}_{j,I_{j,i}} \underline{\mathbf{c}}_{j-1,I_{j,i}}, \tag{48}$$

where

$$\begin{aligned} \underline{\mathbf{c}}_{j,I_{j,i}} &= \left(c_{j-1,0}^{2i} \quad c_{j-1,1}^{2i} \quad c_{j-1,0}^{2i+1} \quad c_{j-1,1}^{2i+1}\right)^{t}, \\ \underline{\mathbf{c}}_{j-1,I_{j,i}} &= \left(c_{j-1,0}^{i} \quad c_{j-1,1}^{i}\right)^{t}, \\ \underline{\mathbf{H}}_{j,I_{j,i}} &= \begin{pmatrix} h_{j,0}^{2i,0} & h_{j,0}^{2i,1} & h_{j,0}^{2i+1,0} & h_{j,0}^{2i+1,1} \\ h_{j,1}^{2i,0} & h_{j,1}^{2i,1} & h_{j,1}^{2i+1,0} & h_{j,1}^{2i+1,1} \end{pmatrix}. \end{aligned} \tag{49}$$

The matrix $\mathbf{H}_{j,I_{j,i}}$ is then easily generalized to the complete sequence

$$S_j : \mathbf{H}_j = \begin{bmatrix} \mathbf{H}_{j,I_{j,0}} & [0] & [0] & [0] \\ [0] & \mathbf{H}_{j,I_{j,1}} & [0] & \vdots \\ \vdots & [0] & \ddots & [0] \\ [0] & [0] & [0] & \mathbf{H}_{j,I_{j,n}} \end{bmatrix}. \tag{50}$$

The previous equation relative to the bounded interval becomes

$$\begin{aligned} \underline{\mathbf{c}}_j &= \mathbf{H}_j \underline{\mathbf{c}}_{j-1} \quad \text{where } \underline{\mathbf{c}}_j = \left(\underline{\mathbf{c}}_{j,I_{j,0}} \quad \underline{\mathbf{c}}_{j,I_{j,1}} \quad \cdots\right)^{t}, \\ \underline{\mathbf{c}}_{j-1} &= \left(\underline{\mathbf{c}}_{j-1,I_{j-1,0}} \quad \underline{\mathbf{c}}_{j-1,I_{j-1,2}} \quad \cdots\right)^{t}. \end{aligned} \tag{51}$$

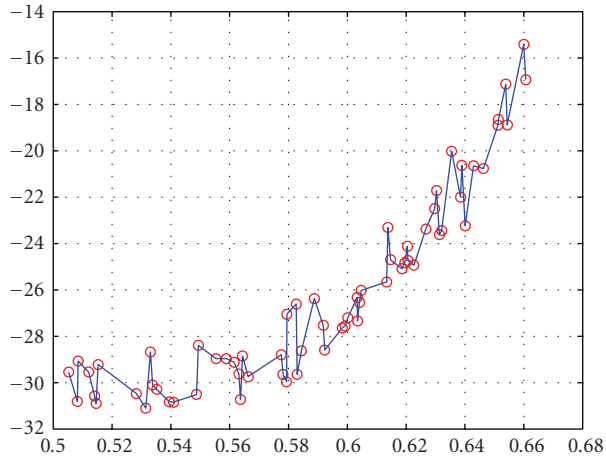

FIGURE 11: Original signal irregularly subsampled.

The details coefficients, after some manipulations, satisfy the following equation:

$$d_{j,k}^{m} = \sum_{l=2i}^{2i+1} \sum_{n=0}^{1} g_{j,k}^{l,n} c_{j-1,k}^{l} \quad \text{for } k = 0, 1;\ m = 2i, 2i+1; \text{ and all } i \in N. \tag{52}$$

Using the same notation as the matrix decomposition $\mathbf{H}_{j,I_{j,i}}$, the computation of the detail coefficients at resolution j, on the bounded interval $I_{j,i}$, are given as follows:

$$\underline{\mathbf{d}}_{j,I_{j,i}} = \mathbf{G}_{j,I_{j,i}} \underline{\mathbf{c}}_{j-1,I_{j,i}} \quad \text{where } \underline{\mathbf{d}}_{j-1,I_{j,i}} = \left(d_{j-1,0}^{i} \quad d_{j-1,1}^{i}\right)^{t},$$
$$\underline{\mathbf{G}}_{j,I_{j,i}} = \begin{pmatrix} g_{j,0}^{2i,0} & g_{j,0}^{2i,1} & g_{j,0}^{2i+1,0} & g_{j,0}^{2i+1,1} \\ g_{j,1}^{2i,0} & g_{j,1}^{2i,1} & g_{j,1}^{2i+1,0} & g_{j,1}^{2i+1,1} \end{pmatrix}. \tag{53}$$

The extension of the matrix decomposition $\mathbf{G}_{j,I_{j,i}}$ to the sequence $\mathbf{S}_j$ is obviously deduced as $\mathbf{H}_{j,I_{j,i}}$. Since the decomposition is orthogonal, the reconstruction matrices are deduced from the decomposition matrices. The decomposition matrices $\mathbf{H}_j$ and $\mathbf{G}_j$ are sparse matrices. Therefore, the decomposition and reconstruction steps will be efficient since efficient algorithms for multiplying a sparse matrix with a vector exist.

Simulation results of the theoretical orthogonal decomposition are provided below. The curve in Figure 11 presents the original signal irregularly subsampled on which the provided simulations are carried out. The samples of the signal are marked by the symbol "∘." Figure 12 presents approximation signals (left graphs of (a), (b), (c), (d), and (e)) and detail signals (right graphs of (a), (b), (c), (d), and (e)) corresponding to five resolution levels $j = 1, 2, 3, 4, 5$ using Haar wavelet and scaling functions given in Sections 3 and 4. For each graphs plotted in (a), (b), (c), (d), and (e), the following symbols "∘," "∗," and "+" represent, respectively, (i) the subsampled data corresponding to the knots of the sequence S_j, (ii) the approximation signals at different resolution level j and (iii) the detail signals at different resolution level j. Simulation results show that, while being in the framework of irregularly spaced data, the behavior of the multiresolution analysis is exactly the same as in the traditional case (regularly spaced data). One can notice that the detail signal variance is smaller than the approximation signal variance. Moreover, the computations show that the detail signal variances increase when going from resolution level $j-1$ to j.

6. CONCLUSION

The main objective of this paper is to provide the required tools for achieving a multiresolution analysis in the specific context of irregularly spaced data. In this environment, the presented work shows that the construction of orthonormal spline scaling and wavelet bases remains always possible. The construction of the bases is carried out in the multiresolution concept exploiting the orthogonal decomposition approach.

The basic tool of this paper is the nonuniform B-spline function. This function presents many interesting properties such as explicit and generalized expression whatever the degree of the spline function when imposing a particular multiplicity on each knot of the initial sequence. In this case, the support of the B-spline is reduced to two consecutive knots in the sequence.

The orthonormalization process of the basic spline basis is performed with the classical Gram-Schmidt method on each bounded intervals of the initial sequence. The paper provided a generalization of the orthonormal spline scaling and wavelet bases construction whatever the degree of the spline function. Our study proves that the scaling and wavelet functions are not, respectively, given by dilating and translating a unique prototype function as in the traditional case. The traditional filter banks are replaced by a set of filters depending on the localization of the samples in the sequence. When the degree of the spline function increases, the number of freedom degrees increase offering thus flexibility in the design of the wavelet functions. It is possible to ensure desirable features such as the continuity of the wavelet function and its successive derivatives. The complete process of decomposing and reconstructing a signal irregularly sampled is provided. The orthogonal decomposition, applied to signals irregularly subsampled, shows that the traditional multiresolution analysis behaviour is respected.

Increasing the degree of the spline function allows circumventing the discontinuity problem of the scaling and wavelet functions at the cost of a very high computational complexity. The number of the scaling and wavelet functions to handle becomes very high. Consequently in future investigation, a great importance will be attached to this crucial problem.

A generalization of the proposed method to the two-dimensional wavelet transform will be studied. The problems involved in the topic of data compression using nonuniform scaling and wavelet functions are interesting to be considered in future investigations.

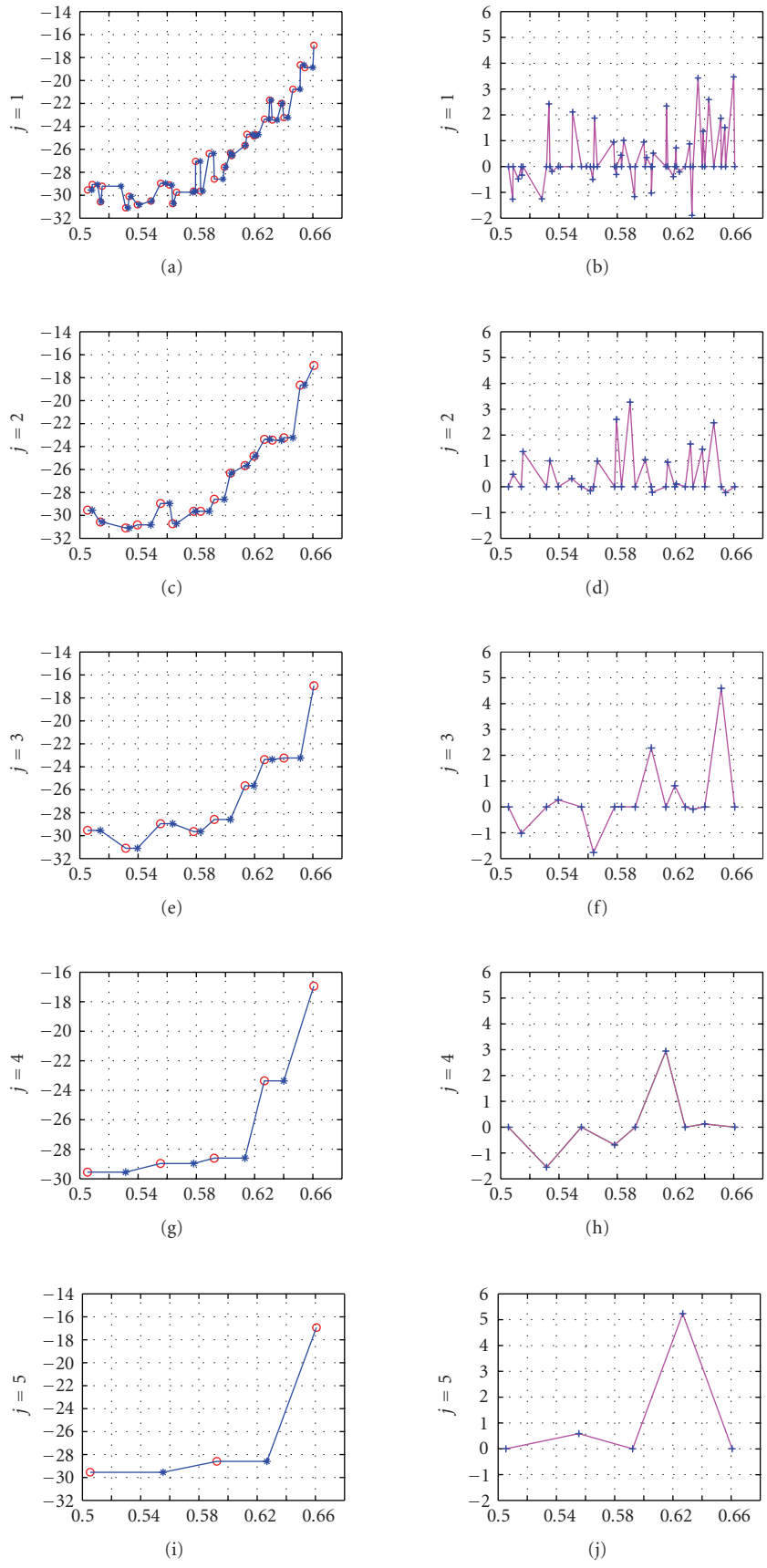

Figure 12: Multiresolution analysis on five resolution levels using Haar scaling and wavelet functions.

ACKNOWLEDGMENT

The authors would like to thank Professor Pierre Duhamel for many interesting and helpful discussions.

REFERENCES

[1] S. Mallat, *A Wavelet Tour of Signal Processing*, Academic Press, San Diego, Calif, USA, 2nd edition, 1999.
[2] M. Vetterli and J. Kovacevic, *Wavelets and Subband Coding*, Prentice Hall, Englewood Cliffs, NJ, USA, 1995.
[3] C. K. Chui, Ed., *Wavelets: A Tutorial in Theory and Applications*, Academic Press, San Diego, Calif, USA, 1993.
[4] O. Rioul and P. Duhamel, "Fast algorithms for wavelet transform computation," in *Time-Frequency and Wavelets in Biomedical Signal Processing*, M. Akay, Ed., chapter 8, pp. 211–242, Wiley-IEEE Press, New York, NY, USA, 1997.
[5] M. D. Buhmann and C. A. Micchelli, "Spline prewavelets for non-uniform knots," *Numerische Mathematik*, vol. 61, no. 1, pp. 455–474, 1992.
[6] I. Daubechies, I. Guskov, P. Schröder, and W. Sweldens, "Wavelets on irregular point sets," *Philosophical Transactions of the Royal Society of London. A*, vol. 357, no. 1760, pp. 2397–2413, 1999.
[7] I. Daubechies, I. Guskov, and W. Sweldens, "Commutation for irregular subdivision," *Constructive Approximation*, vol. 17, no. 4, pp. 479–514, 2001.
[8] T. Lyche, K. Mørken, and E. Quak, "Theory and Algorithms for non-uniform spline wavelets," in *Multivariate Approximation and Applications*, N. Dyn, D. Leviatan, D. Levin, and A. Pinkus, Eds., pp. 152–187, Cambridge University Press, Cambridge, UK, 2001.
[9] C. De Boor, *A Practical Guide to Splines*, Springer, New York, NY, USA, revised edition, 2001.
[10] G. Farin, *Curves and Surfaces for CAGD*, Morgan-Kaufmann, San Fransisco, Calif, USA, 5th edition, 2001.
[11] N. Chihab, A. Zergaïnoh, P. Duhamel, and J. P. Astruc, "The influence of the non-uniform spline basis on the approximation signal," in *Proceedings of 12th European Signal Processing Conference (EUSIPCO '04)*, Vienna, Austria, September 2004.
[12] M. A. Unser, "Ten good reasons for using spline wavelets," in *Wavelet Applications in Signal and Image Processing V*, vol. 3169 of *Proceedings of SPIE*, pp. 422–431, San Diego, Calif, USA, July 1997.

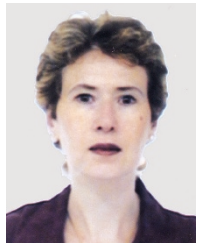

Anissa Zergaïnoh received the State Engineering degree in electrical engineering from National Telecommunication School in 1989, the M.S. degree in information technology in 1990, and the Ph.D. degree in 1994 all from University Paris 11, Orsay, France. From 1992 to 1994, she worked at the National Institute of Telecommunications (INT, Evry, France) where her research activities were on digital signal processing, fast filtering algorithms, and implementation problems on DSP. Since 1997, she is Associate Professor at Galilée Institute of University Paris 13, France. From 2005 to 2007, she joined the CNRS/LSS laboratory, Supélec, Orsay, France as a Visiting Professor. Her current research interests include image and video compression, image reconstruction, irregular sampling, interpolation, and wavelet transforms.

Najat Chihab received her M.S. degree in information technology from University Paris 11, France in 2001. She received the Ph.D. degree from the University Paris 13, France in 2005. Her research interests focus on nonuniform B-spline function, interpolation, approximation, irregular subsampling, and multiresolution analysis.

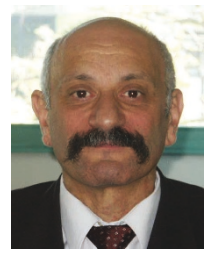

Jean Pierre Astruc was born in France in 1953. He received the Dr.Ing. degree in 1979 and the Doctorat es Sciences degree in physics in 1987 both at University Paris 13, France. His first research interests were in the energy transfer between atoms and molecules. Since 1992, he is Professor at University Paris 13, France. From 1988 to 1998 he founded a working group of experience's control in the LIMHP/CNRS Laboratory at University Paris 13, France. His research activities were concentrated on the measurements of the critical parameters of a pure fluid by expert system and on the experiments control using image processing. He joined the L2TI Laboratory of Galilée Institute, University Paris 13 in 1998. Since 2002, he is the Head of the Galilée Institute. His current research interests include image and video compression.